ISSN: 2414-1895 DOI: 10.6919/ICJE.202507_11(7).0022

Design on an Autonomous Navigation and Sampling System for Multipurpose Monitoring Vessels in River Systems

Kambale Mughanda[1], Huli Niu[2,*], Xiongfei Yan[2], Jiarui Guo[3], Zhenduo Yang[3], Jiachao Wen[2], and Jimeng Zheng[3]

[1] School of International Education, Hebei University of Science and Technology, Shijiazhuang, China

[2] School of Mechanical Engineering, Hebei University of Science and Technology, Shijiazhuang, China

[3] College of environmental science and engineering, Hebei University of Science and Technology, Shijiazhuang, Hebei 050018, China

[*]Corresponding author: 251171741@qq.com

Abstract

Currently, water sample collection and environmental monitoring in river basins primarily rely on manual operations. These methods suffer from issues such as low efficiency, high labor intensity, and insufficient real-time data acquisition, making it difficult to meet the complex monitoring demands of river basin environments. To address these challenges, this study designed a smart multi-purpose monitoring vessel system for river travel and sampling. The system aims to achieve autonomous navigation and automatic water sampling in diverse river basins, thereby reducing manual intervention and improving monitoring efficiency and data accuracy. The design process encompassed the development of the system's principle, workflow, motion control, and overall structural designs. Detailed calculations and analyses of key process parameters were conducted. Digital modeling methods were employed for static analysis and optimization of the mechanical structure. The results demonstrate that the designed system can effectively enhance the automation level and operational efficiency of monitoring and sampling in complex aquatic environments. It provides stable and reliable technical support for river basin water ecological monitoring, pollution prevention, water quality management, and resource management.

Keywords

River Monitoring Systems; Multi-Purpose Monitoring Vessel; Autonomous Water Sampling; Automated Monitoring; System Design.

1. Introduction

With the rapid development of the socio-economy, the protection of the aquatic ecological environment faces enormous challenges. In the field of watershed water environment monitoring [1], traditional sampling methods primarily rely on manual operations, which have many drawbacks. On the one hand, manual sampling is inefficient, labor-intensive, and struggles to meet the high-frequency, multi-point requirements of complex watershed environmental monitoring. Especially in complex waters such as urban rivers, marshes, and ponds [2], the difficulty and risk of manual sampling are significantly increased. On the other hand, manual sampling lacks real-time capability, making it unable to reflect the dynamic changes of the water environment in a timely manner and

ISSN: 2414-1895 DOI: 10.6919/ICJE.202507_11(7).0022

difficult to meet the real-time data requirements of modern aquatic ecological monitoring, pollution prevention, and resource management [3-4]. In addition, manual sampling also suffers from problems such as significant sampling errors and compromised data accuracy, ultimately affecting the reliability of monitoring results and the effectiveness of scientific decision-making.

To address the aforementioned issues and enhance the automation level and operational efficiency of watershed water environment monitoring, scholars and enterprises worldwide have conducted extensive research. Banerjee B P et al. [5] developed an integrated electromechanical and pneumatic system mounted on a drone to remotely collect water samples from tailings ponds, thereby improving monitoring efficiency and safety. Gardner W S et al. [6] described a system that used a synchronous motor driving an overflow pipe to achieve periodic water sample collection. This method offers advantages such as low cost and avoiding sample contamination through contact only with glass or Teflon components. However, it may be less adaptable to complex water quality conditions in practical field applications and requires high maintenance. Parmar et al. [7] explored gear design optimization using the NSGA-II algorithm, specifically examining the impact of gear bonding on the multi-objective optimization of planetary gear mass and efficiency. Yokota et al. [8] achieved a reduction in gear pair mass by using mass as the optimization objective, macro parameters as design variables, and fatigue strength and geometric dimensions as constraints. Schwarzbach et al. [9] utilized a helicopter-type drone equipped with a small water pump connected to a 1.5m long suction pipe to collect water samples (~500ml) into a sampling bottle. They also studied the stability of the drone under disturbances such as gusts and payload variations. Ore et al. [10] used a quadrotor drone equipped with a micro pump to obtain small-volume water samples (≤25ml), achieving a flight time of up to 20min. Cengiz et al. [11] designed a drone sampler featuring a retractable sampling tube capable of collecting ~130ml samples, primarily applied to lake water collection, but limited by short endurance and flight distance. Furthermore, according to relevant literature, manual collection remains the prevalent method for river sediment sampling.

This study addresses the practical needs of environmental monitoring in complex river basins by designing a smart multi-purpose monitoring vessel system for autonomous navigation and sampling. The system integrates three major functional modules: water column sampling, sediment sampling, and sample storage/handling. Through modular design, automated process control, and digital analysis for optimization, it achieves autonomous navigation, precise positioning, and automatic water column and sediment sampling in various river basins. This study aims to provide an efficient, precise, and reliable automated monitoring solution for river basin water ecological monitoring, pollution prevention, and resource management. It seeks to promote the advancement of intelligent water environment monitoring technology and contribute to the protection and restoration of aquatic ecosystems.

2. Overall Design of the Traveling and Sampling Equipment for Multi-Purpose Monitoring Vessels

2.1 Differences in Aquatic Environments and Collection Requirements

Through consulting relevant materials and conducting surveys on related enterprises [12], it is found that multi-purpose monitoring vessels need to adapt to the characteristics of different water environments during their practical application. The relevant information is presented in Table 1.

During the sampling process of water samples, the volume of collected water should not be less than 250 milliliters. The sampling container should be a polyethylene plastic bottle or a hard glass bottle, with a capacity of over 500 milliliters. When conducting stratified sampling of water bodies, it should be carried out from top to bottom to avoid mixing of water from different layers. During sampling, the sediment at the bottom of the water should not be stirred, ensuring that the sampling error is controlled within ±5%.

ISSN: 2414-1895 DOI: 10.6919/ICJE.202507_11(7).0022

Table 1. Differences in water environment morphology for navigation of ulti-purpose monitoring vessels

Surface water environment	Boundary shape	Depth range	velocity of flow	Underwater conditions	Vegetation cover
Urban river channel	Straight line or curved polygonal line	Relatively stable	Have a certain flow rate	Flat, gravel or concrete, with debris	low
swamp	The boundary is blurry and irregular	Significant changes	The flow rate is low, almost static	Soft and muddy soil, with potholes	tall
pond	Diverse shapes	Small changes	Weak flow velocity	Relatively flat, with a mixture of sediment and humus	centre

When conducting sediment sampling, the sediment sampler should be made of high-strength material with good wear resistance and corrosion resistance, and the sediment sampling volume should be controlled between 0.5-1.0kg. The sediment sampling points should avoid areas with riverbed scouring, unstable sediment deposition, lush waterweeds, and easily disturbed surface sediment. The sample volume retention rate should be ≥95%. The equipment should operate in a fully automatic mode, with remote manual switching operation and fault warning functions, and should produce low noise and consume little energy during navigation and sampling.

2.2 Process Flow Design

The overall design of the multifunctional monitoring vessel equipment is based on an in-depth analysis of process requirements. Only after we clearly understand the process requirements can we ensure that the designed monitoring vessel meets the specific needs during the collection process, thereby achieving the goals of improving accuracy, reducing labor costs, and optimizing product quality. The equipment adopts a modular design concept, with standardized modules for each function, to design the ideal product equipment. The sediment collection module and water sample collection module each complete specific tasks without interfering with each other, and the collection module completes the collection tasks of sediment and water samples. Each process is automated, requiring no manual operation. The basic process flow is shown in Fig. 1.

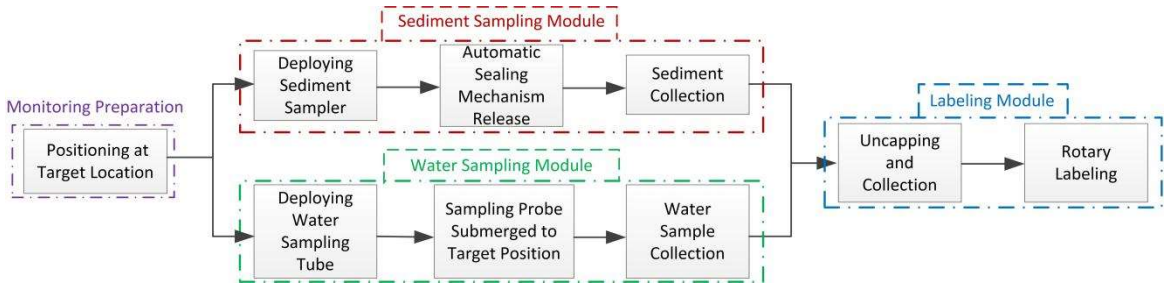

Fig. 1 Process flow diagram of monitoring vessel traveling and sampling

3. Overall Design of Walking and Sampling Equipment for Multifunctional Monitoring Vessels

3.1 Process Flow Diagram Design

The drone transports the sampling bottle and turntable to the monitoring vessel, which then performs path planning according to the preset sampling target and moves to the sampling position. Water

ISSN: 2414-1895 DOI: 10.6919/ICJE.202507_11(7).0022

sampling is carried out, with the winch vertically lowering the sampling tube to the preset depth. The centrifugal pump is activated to collect water samples through the sampling tube. Next, the sampling bottle moves to the stopper removal and insertion station I, where the mechanical gripper removes the bottle stopper. The sampling bottle then moves to the water sample canning station III, where the canning port opens and canning begins. The water sample is vertically injected into the sampling bottle. After the water sample is canned, the sampling bottle moves back to the stopper removal and insertion station I. The mechanical gripper descends vertically to press the bottle stopper smoothly into the sampling bottle. The sealed sampling bottle moves to the marking station IV, where the laser marking device is activated to drive the laser marking head to perform rotary movement, completing the marking of the sampling bottle.

For sediment collection, the crane uses a cable to vertically lower the columnar sampler to the riverbed surface. The micro motor equipped on the columnar sampler starts, driving the spiral drill bit to rotate and cut for soil collection. Then, the sediment sampling container moves to the soil canning station II. The crane column rotates to align the sampler with the container opening, allowing the soil sample to fall into the container for soil canning. After canning is completed, the sediment sampling container moves to the marking station IV. The laser marking device starts, driving the laser marking head to move along the circular guide rail, completing the marking of the sampling container.

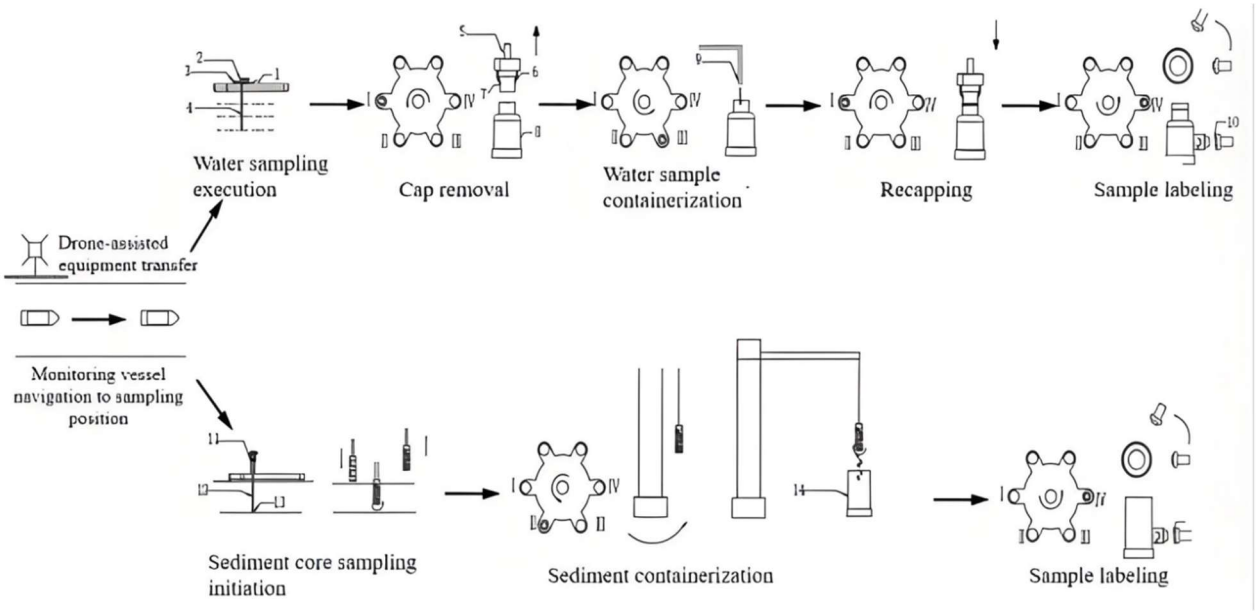

Fig. 2 Process flow diagram of the traveling and sampling system of the multi-purpose monitoring vessel for smart river channels

3.2 Design of Water Sample Collection Module

After reaching the sampling target, the winch lowers the sampling tube and starts the sampling centrifugal pump [13]. Based on the principle of centrifugal force, the impeller rotates, and the blades stir the water, causing it to be thrown towards the edge under the action of centrifugal force. A low pressure is formed at the center of the impeller, and under the action of atmospheric pressure, external water is drawn in through the sampling hose, achieving water sample collection. As shown in Fig. 3.

ISSN: 2414-1895 DOI: 10.6919/ICJE.202507_11(7).0022

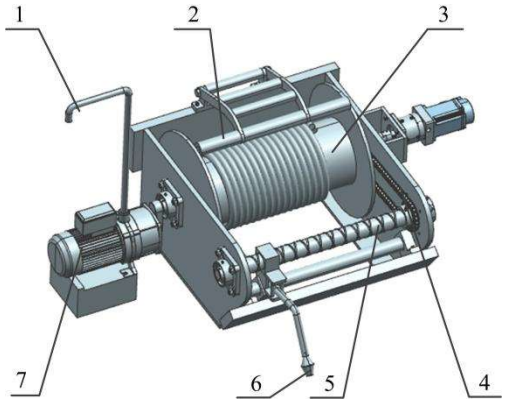

1. Sampling tube; 2. Guide pressure roller; 3. Winch drum; 4. Hinge; 5. Drive shaft; 6. Filter head; 7. Multistage centrifugal pump in bedroom

Fig. 3 Water sample collection system

3.3 Design of Sediment Collection Module

Upon reaching the sampling target, the crane lowers the sampler to the water bottom via a cable. The cylindrical sampler utilizes a micro motor to drive the drill rod, which crushes the sediment on the water bottom through a rotational cutting principle, allowing the sediment to enter the cylindrical sampler. The sampling is sealed through a sealing valve structure, achieving bottom sediment collection. As shown in Fig. 4.

The sediment sampler consists of a rotary motor and a reducer, which are connected to the drill rod via a spline shaft sleeve, driving the spiral drill rod to rotate. The feed motor drives the ball screw through a coupling, and the nut seat, through a connecting mechanism, drives the drill rod to complete the lifting and lowering motion. Meanwhile, the sealing structure at the bottom is realized through a sealing switch and a spring mechanism.

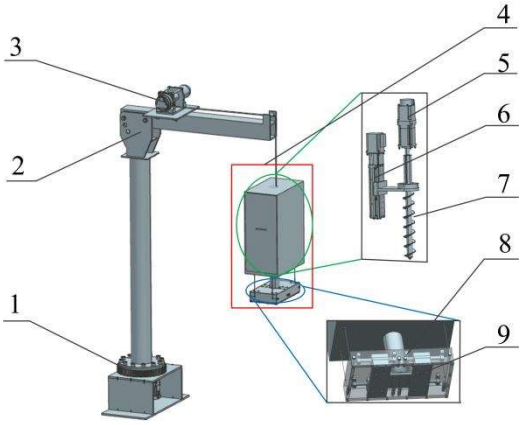

1. Bottom rotary table; 2. Suspension frame; 3. Rope winch; 4. Sampler; 5. Rotary drive; 6. Lifting drive; 7. Auger rod; 8. Bottom sediment collection bin; 9. Sealed switch

Fig. 4 Sediment collection system

3.4 Design of Sample Collection Module

(1) As shown in Figure 4.1, the calculation formula for the pressing force of the bottle stopper is:

$$F = \frac{\rho \times \pi (d_1 + d_2) \times L \times \mu}{2 con \alpha} \tag{1}$$

ISSN: 2414-1895 DOI: 10.6919/ICJE.202507_11(7).0022

In the formula, *F* represents the bottle stopper pressing force (N); *p* represents the contact pressure (N/mm²); d1 and d2 represent the diameters of the small and large ends of the bottle stopper (mm), taking values of 56mm and 46mm respectively; L represents the bonding length (mm), taking a value of 14.14mm; u represents the friction coefficient, which is 0.5; a represents the half angle of the conical surface, which is 8.13°

Formula for calculating contact pressure p:

$$P = \frac{E \times \delta \times \tan \alpha}{d \times \left(1 - v^2\right)} \tag{2}$$

In the formula, E represents the elastic modulus of the material (mPa), ranging from 0.5 mPa to 1 mPa; δ represents the axial indentation (indentation depth), which is 14 mm

a - half angle of conical surface 8.13°; d - average diameter at contact point (mm) 50 mm; v - Poisson's ratio 0.5

When the elastic modulus E is 0.5, the calculated pressing force F on the bottle stopper is 30.34N;

When the elastic modulus E is equal to 1, the calculated pressing force F on the bottle stopper is 60.67N.

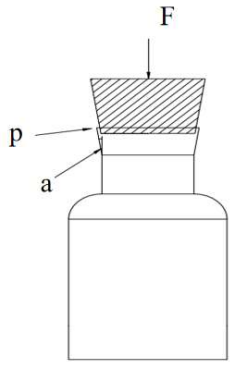

Fig. 5 Schematic diagram of bottle stopper pressing

(2) As shown in Figure 4.2, the calculation formula for the clamping force of the mechanical gripper is:

$$F = \frac{mgs}{2\mu \cos \alpha} \tag{3}$$

In the formula, m represents the mass of the bottle stopper in kilograms, set to 0.1kg; g denotes the acceleration of gravity, set to 10g/m^3; s signifies the safety factor, ranging from 3 to 5; u stands for the friction coefficient, set to 0.3;θ and φ represents the half angle of the conical surface (half of the conical angle θ)

When the safety factor s is 3, the calculated clamping force F of the bottle stopper is 5.05N;

When the safety factor s=5, the calculated bottle stopper clamping force F=8.42N.

ISSN: 2414-1895 DOI: 10.6919/ICJE.202507_11(7).0022

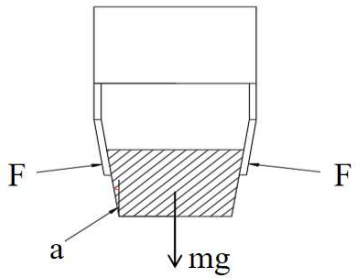

Fig. 6 Schematic diagram of bottle stopper clamping

It is mainly composed of a sample collection container rotary table, a capping mechanism, and a marking mechanism. The rotary drive system consists of a servo motor, a reducer, and a coupling, which drives the pulley to rotate, thus achieving the rotation of the sample collection container platform. The uncapping mechanism is mainly composed of an air cylinder and a pneumatic mechanical claw. First, the uncapping mechanism opens the bottle cap, the rotary platform rotates counterclockwise, and then the sludge sample collected by the sediment collection device is transferred into the sample collection container. It continues to rotate counterclockwise to the next station, where the water sample collected by the water sampling device is transferred into the sample collection container. After completing the two sample transfers, the motor reverses, and the open sample collection container is rotated until the uncapping mechanism completes the sealing. The same operation is repeated for the next sample collection container. When the sample-filled sample collection container rotates to the marking mechanism, the motor drives the pinion to drive the gear wheel, which in turn drives the marker to rotate counterclockwise. The marking is completed, the motor reverses, and the marker returns to its initial position.

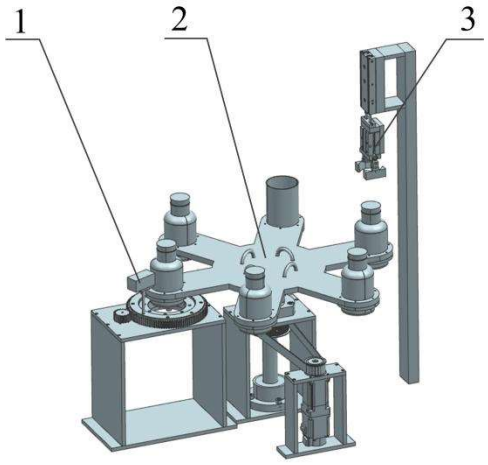

1. Marking mechanism; 2. Intermittent rotary table for sample collection containers; 3. Stopper insertion mechanism

Fig. 7 Sample collection system

The components for removing and inserting plugs of sampling bottles on monitoring ships facilitate the operation of removing and inserting plugs during water quality sampling. Due to the uniform model and specifications of sampling bottles, the execution of actions forms a standardized process: in the Tk stage, the clamping jaw moves vertically downward; in the Ts stage, the clamping jaw grasps the bottle plug; in the Td stage, after completing the action of removing and lifting the plug, it resets to a safe height; in the To stage, the clamping jaw grasps the bottle plug and remains stationary at the initial height, waiting for the sampling bottle to be labeled and then rotates back to the initial position; in the Tk' stage, it moves vertically downward to install the bottle plug; in the Ts' stage, the

ISSN: 2414-1895 DOI: 10.6919/ICJE.202507_11(7).0022

clamping jaw releases the bottle plug; in the Td' stage, the clamping jaw lifts to the initial position, completing the entire cycle. As shown in Fig. 8.

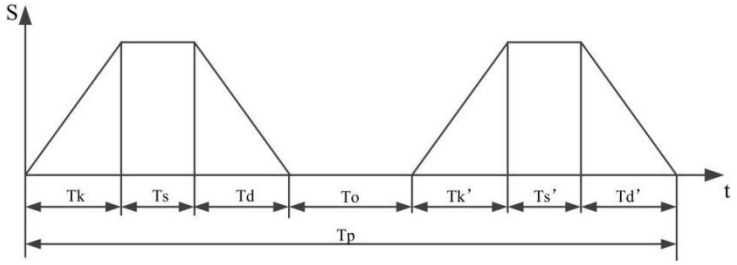

Fig. 8 Movement of the mechanism for removing and inserting the stopper of the sampling bottle

The intermittent rotary table for sample collection containers facilitates the positional movement of sampling containers during the sampling process on a monitoring vessel. The disc is equipped with six positioning slots, and there are four functional stations around the disc: water sample canning station, sediment canning station, sampling bottle stopper removal/insertion station, and labeling station. This allows the sampling containers to move between different stations. The entire motion process is divided into the following stages: Tk stage for opening the stopper by the stopper mechanism; Ts stage for the rotary table to rotate counterclockwise by 60° driven by a stepper motor to complete the station switching; Td stage for depositing sediment; Ta stage for the rotary table to rotate counterclockwise by 120° to reach the labeling mechanism; Tc stage for labeling; Tb stage for returning to the initial position; and To stage for the stopper mechanism to install the bottle stopper, completing the entire process. As shown in Fig. 9.

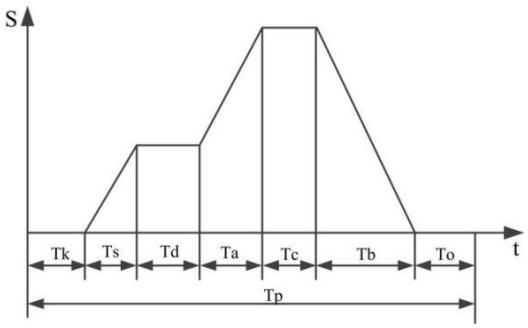

Fig. 9: Motion diagram of intermittent rotary table for sample collection container

3.5 Overall Presentation of Mechanical System

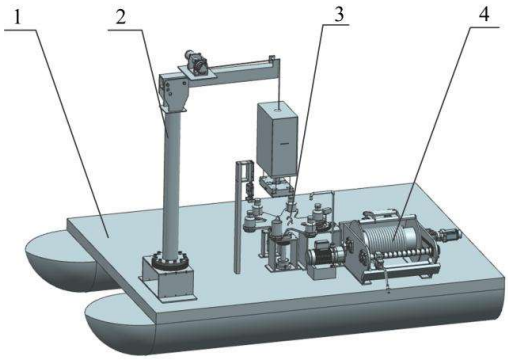

1. Monitoring vessel hull; 2. Sediment collection system; 3. Sample collection system; 4. Water sampling system

Fig. 10 Structural diagram of the walking and sampling equipment of the multi-purpose monitoring vessel

ISSN: 2414-1895 DOI: 10.6919/ICJE.202507_11(7).0022

The sediment sampling system, water sampling system, and sample collection system are placed on the monitoring vessel separately. Both sediment samples and water samples are placed in the sample collection system. Other parts of the monitoring vessel include a vegetation arrangement system, which is not studied in this research. As shown in Fig. 10.

4. Digital Analysis of Key Components of Monitoring Ship's Navigation and Sampling Equipment

4.1 Model Statics Analysis

The fixture connection block structure studied is the assembly mechanism for various components of the assembly machine. It is a key structure for the assembly machine to complete assembly and a crucial component for achieving continuous work at each station. Therefore, the accuracy of the connection block structure directly affects the accuracy of assembly. In order to ensure that the connection block can meet assembly requirements while optimizing its shape during the design process, the rationality of the design is verified by analyzing the results of changes in shape before and after. Firstly, a linear statics analysis of the connection block is required, and the process is as follows:

(1) Simplification of the model: This design utilizes SW software to create a 3D CAD model. To ensure reliability and analytical accuracy while reducing unnecessary computational workload and enhancing the speed of finite element analysis, the model undergoes simplification in the following ways. The main simplifications include: 1) Removal of small feature areas such as bolt holes, fixture holes, and non-stressed mounting holes; 2) Simplification of force-bearing holes into cylindrical shapes due to the vertical downward force applied by the cylinder to the connecting block. The simplified model is illustrated in Fig. 11.

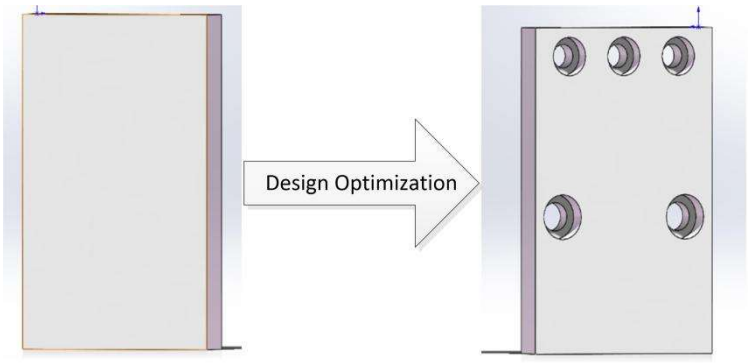

Fig. 11 Comparison of model simplification

(2) Material property definition: Common engineering materials are provided in the material library of SW. The material used for the connecting block model here is aluminum alloy 6061, with a new designation of 2A11. The material parameters are shown in Table 2.

Table 2. Parameter Table of Aluminum Alloy 6061

material	Density (g/cm^3)	Elastic modulus / (GPa)	Yield strength / (MPa)	Poisson's ratio
aluminium alloy	2.7	69	270	0.33

(3) Grid generation: The quality and density of the grid directly affect the accuracy of the calculation results in SW software. There are mainly three types of grid generation methods: free mesh generation, mapped mesh generation, and adaptive mesh generation. Due to the simple and regular structure of

ISSN: 2414-1895 DOI: 10.6919/ICJE.202507_11(7).0022

the connecting plate, free mesh generation is adopted here. This method allows for random mesh generation based on the shape and boundary of the model, generating tetrahedral or hexahedral elements and meshing the connecting block, as shown in Fig. 12.

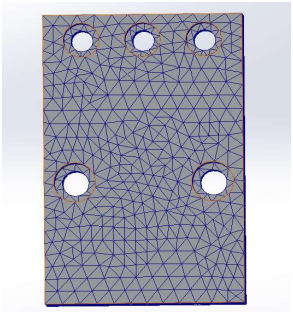

Fig. 12 Grid division diagram

(4) Add fixed constraint: The connecting plate is fixed on the parallel air claw. According to the analysis of the degree of freedom of the sheet metal, the connecting plate only experiences tangential force. Therefore, a planar constraint is added to the connecting plate, specifically at the central hole.

(5) Load application: For safety reasons, force is applied to the connecting plate based on the most dangerous scenario. According to the previous text, it is known that the connecting block is subjected to a vertical downward force from the parallel air claw when it is at rest. Based on the analysis of the number of motion actions at each of these two workstations, it is determined that they do not press down simultaneously. Therefore, the higher force is applied for load application through analysis.

The pneumatic gripper needs to grasp the bottle stopper stably to avoid the stopper falling off due to insufficient clamping force, or deforming or overloading the pneumatic gripper due to excessive clamping force. A pneumatic gripper with a theoretical output force of 22.6N is selected, and the actual clamping force is limited to a range of 10~15N through a throttle valve (considering both safety and flexibility protection). Through comparative analysis, the applied load is 20N, and its load application is shown in Fig. 13.

Fig. 13 Load distribution diagram

(6) Solution calculation and post-processing of results: After completing the above operations, calculation analysis can be carried out. The total deformation and stress changes of the connected block structure after calculation are shown in Fig. 14. The maximum total deformation is 0.029988mm, which is less than the required maximum deformation of 0.05mm. The maximum stress value is 1.3635MPa, which is much lower than the yield strength value of hard aluminum LY11. Therefore, both meet the requirements.

ISSN: 2414-1895 DOI: 10.6919/ICJE.202507_11(7).0022

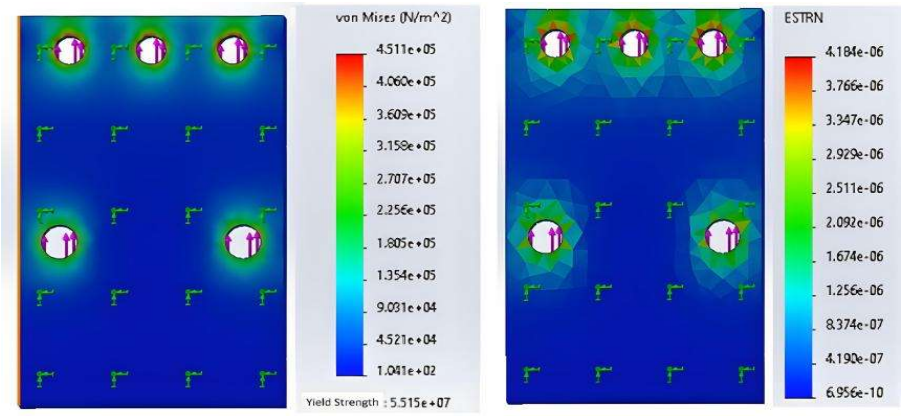

Fig. 14 Total deformation and stress contour plot

4.2 Model Optimization Analysis

Conduct a statics analysis on the structure of the fixture connection block, optimize its shape while meeting the requirements, and perform modeling optimization in SW software by removing material from the model. Chamfer the solid connection block, ensuring that all corners on the connection block are chamfered for ease of installation. The simplified models of the connection block before and after optimization are shown in Fig. 15.

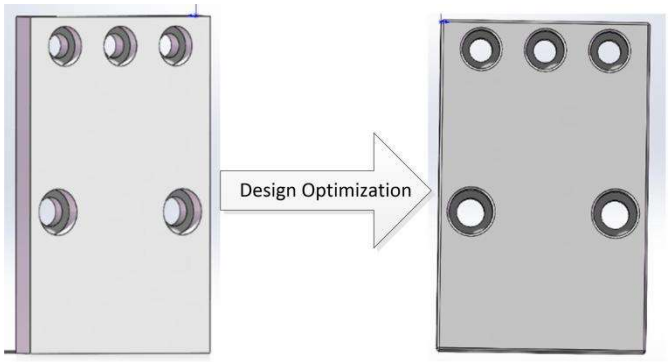

Fig. 15 Optimized Simplified Model

Similarly, a finite element analysis was conducted on the optimized model to assess its compliance with the requirements. A maximum force of 20N was applied to the optimized connecting block, and through computational analysis, the total deformation and stress changes of the connecting block structure after calculation are shown in Fig. 16.

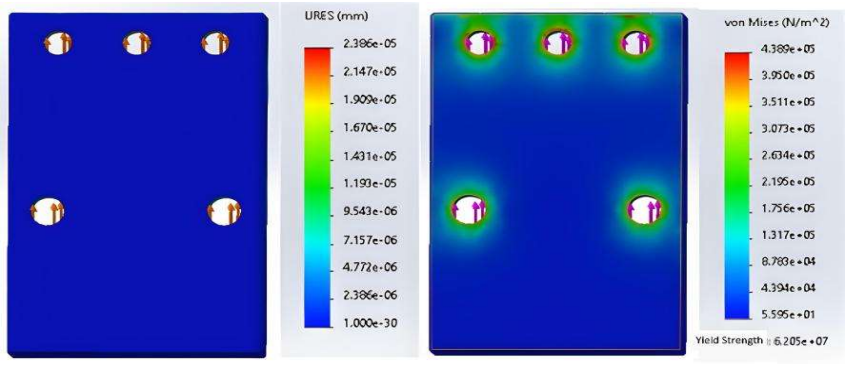

Fig. 16 Total deformation and stress contour plot

ISSN: 2414-1895 DOI: 10.6919/ICJE.202507_11(7).0022

Table 3. Comparison of Results and Parameters

model	Total Deformation/mm	Equivalent Stress/MPa	Weight/kg
model	0.029	1.47	0.5
optimization	0.047	1.51	0.5

Through statics analysis and topology optimization analysis of the connecting block, it is determined that the deformation of the connecting block according to assembly requirements cannot exceed 0.05mm. The deformation before and after optimization is less than 0.05mm, and the stress changes before and after optimization are both much smaller than the yield strength value of aluminum alloy, which is 270MPa. Therefore, the requirements are met.

5. Conclusion

This study addresses the issues of low efficiency, poor safety, and insufficient real-time data collection in traditional manual water sampling. It designs a smart river multi-purpose monitoring vessel navigation and sampling system. Through the integrated design of system principles, process schemes, motion control, and mechanical structures, combined with mechanical analysis and digital verification of key parameters, the following innovative achievements have been realized:

Modular system architecture: Three major functional modules, namely water sampling, sediment sampling, and sample processing, have been constructed. Water sampling utilizes centrifugal pump-driven impeller negative pressure suction technology to achieve stratified sampling. Sediment sampling employs a micro-motor-driven auger rod to rotate and cut, combined with a sealing valve structure to ensure the integrity of sediment samples.

Automated process flow: Based on preset path navigation and precise positioning, it achieves full automation of the entire process, including vertical lowering of sampling tubes, stratified sample injection, bottle stopper pressing, and laser marking. The clamping force of the mechanical gripper has been optimized through mechanical calculations to ensure the stability of bottle stopper operations.

Structural reliability verification: Topological optimization was conducted on key connectors using statics analysis. Under a load of 20N, the maximum deformation of the aluminum alloy 6061 fixture connection block was 0.047mm, with a peak stress of 1.51MPa, meeting the requirements for strength and accuracy.

Environmental adaptability design: The system can adapt to complex water bodies such as urban rivers, marshes, and ponds, with a sampling capacity meeting the specification requirements of water samples ≥250mL and sediment 0.5–1.0kg.

Acknowledgments

The authors gratefully acknowledge the financial support from Research and Practice Project on Innovation and Entrepreneurship Education Teaching Reform in Higher Education Institutions in Hebei Province (2023cxcy088) and Collaborative Education Project of Industry University Research by the Ministry of Education (2410314936 and 2412030712).

References

[1] Li M M, Jiang T, Chen T T, et al. Otolith microchemistry of the estuarine tapertail anchovy Coilia nasus from the Anqing section of the Yangtze River and its significance for migration ecology. Acta Ecologica Sinica, 2017, 37(8): 2788-2795.

[2] Yin Z. Distribution and ecological risk assessment of typical antibiotics in the surface waters of seven major rivers, China. Environmental Science: Processes & Impacts, 2021, 23(8): 1088-1100.

[3] Jiang Y, Li M, Guo C, et al. Distribution and ecological risk of antibiotics in a typical effluent–receiving river (Wangyang River) in north China. Chemosphere, 2014, 112: 267-274.

ISSN: 2414-1895 DOI: 10.6919/ICJE.202507_11(7).0022

[4] Min R,Ma K,Zhang H,et al.Distribution and risk assessment of microplastics in Liujiaxia Reservoir on the upper Yellow River.Chemosphere,2023,320:138031.

[5] Banerjee B P, Raval S, Maslin T J, et al. Development of a UAV-mounted system for remotely collecting mine water samples. International Journal of Mining, Reclamation and Environment, 2020, 34(6): 385-396.

[6] Gardner W S, Campbell J E. Composite Water-Sampling Device. Journal-American Water Works Association, 1967, 59(9): 1187-1189.

[7] PARMAR A, RAMKUMAR P, SHANKAR K. Macro geometry multi-objective optimization of planetary gearbox considering scuffing constraint. Mechanism and Machine Theory, 2020, 154: 104045.

[8] Yokota T, Taguchi T, Gen M. A solution method for optimal weight design problem of the gear using genetic algorithms. Computers & industrial engineering, 1998, 35(3-4): 523-526.

[9] Schwarzbach M, Laiacker M, Mulero-Pazmany M, et al. Remote water sampling using flying robots//2014 International Conference on Unmanned Aircraft Systems (ICUAS). IEEE, 2014: 72-76.

[10] Ore J P, Elbaum S, Burgin A, et al. Autonomous aerial water sampling. Journal of Field Robotics, 2015, 32(8): 1095-1113.

[11] Koparan C, Koc A B, Privette C V, et al. Evaluation of a UAV-assisted autonomous water sampling. Water, 2018, 10(5): 655.

[12] Zhong J C, Ben-Sheng Y O U, Cheng-Xin F A N, et al. Influence of sediment dredging on chemical forms and release of phosphorus. Pedosphere, 2008, 18(1): 34-44.

[13] Wang Y, Liu H Y, Zhang W L, et al. Improvement of Physicochemical Properties in Dredging Areas of Dianchi Lake, China. Advanced Materials Research, 2012, 554: 1952-1956.